DALTON

Some new dipyridyl and diphenol bridging ligands containing oligothienyl spacers, and their dinuclear molybdenum complexes: electrochemical, spectroscopic and luminescence properties

Joachim Hock, Alexander M. W. Cargill Thompson, Jon A. McCleverty * and Michael D. Ward *

School of Chemistry, University of Bristol, Cantock's Close, Bristol BS8 1TS, UK

A series of new ligands has been prepared in which pyridyl (L^1–L^5) or phenol (H_2L^7) end-groups are linked by oligothienyl chains: 2,5-bis(4-pyridyl)thiophene (L^1); 5,5′-bis(4-pyridyl)-2,2′-bithiophene (L^2); 5,5″-bis(4-pyridyl)-2,2′:5′,2″-terthiophene (L^3); 5,5‴-bis(4-pyridyl)-2,2′:5′,2″:5″,2‴-quaterthiophene (L^4); 5,5′-bis[2-(4-pyridyl)ethenyl]-2,2′-bithiophene (L^5) and 5,5′-bis(4-hydroxyphenyl)-2,2′-bithiophene (H_2L^7). The compounds L^1–L^5 undergo two one-electron reductions at potentials which converge as the compounds lengthen; H_2L^7 shows an irreversible oxidation ascribed to the formation of a quinone. They all have very strong π–π* transitions in their electronic spectra and are all strongly luminescent. Attachment of {Mo[HB(dmpz)$_3$](NO)Cl} termini (dmpz = 3,5-dimethylpyrazolyl) to these compounds gives paramagnetic (for L^1–L^5) or diamagnetic (for L^7) dinuclear complexes which show strong electrochemical interactions between the termini. the (formally) 17-electron/18-electron metal-based couples in the complex of L^1, for example, are separated by 450 mV, which may be ascribed to a substantial degree of delocalisation of the added electrons onto the bridging ligands. The electrochemical interactions across the ligands are significantly stronger than across those of comparable length with polyene bridges, which confirms the more effective ability of the oligothienyl groups to transmit electronic interactions. The EPR spectra of the paramagnetic dinuclear complexes of L^1–L^5 reveal the presence of magnetic exchange interactions between the unpaired spins. The complexes are all weakly luminescent, due to residual ligand-based luminescence which is not entirely quenched by the metal centres.

The synthesis of dinuclear complexes in which two redox-active metal groups undergo strong electrochemical interactions across a long, conjugated bridging ligand are of interest for the study of mixed-valence complexes and the eventual development of molecular wires, since a strong electronic coupling between the metal end-groups in model complexes indicates that the bridging wire may have good electron-conduction properties in a nanoscopic circuit.[1,2] We have demonstrated recently that dinuclear complexes of the type [{Mo[HB(dmpz)$_3$](NO)Cl}$_2$(μ-L)] (dmpz = 3,5-dimethylpyrazolyl), in which L is a bridging ligand with pyridyl termini, show exceptionally strong electrochemical interactions between the molybdenum groups[3,4] because a particularly favourable interaction between the metal d_π and bridging ligand π* orbitals allows extensive delocalisation of electrons across the bridge.[5] In addition the two paramagnetic {Mo[HB(dmpz)$_3$](NO)Cl} fragments undergo magnetic exchange interactions,[3,4,6] so we have two quantitative ways of relating metal–metal interactions (electrochemical and magnetic) to the structure and properties of the bridging ligand.

Oligothiophenes have long been known to be particularly effective organic conductors, and as such have attracted wide interest as components of conductive materials, electrooptic and electronic devices, and highly organised molecular assemblies.[7] Their desirable electronic properties have several origins. Each thienyl unit is planar and therefore more rigid than a butadienyl unit which has conformational flexibility and can exist as both cisoid and transoid conformers. A chain of α-coupled thienyl units is more likely to be coplanar than, for example, a polyphenylene chain because of the decreased steric interaction between the H^3/H^4 protons of adjacent rings compared to the analogous H^2/H^6 steric interaction in polyphenyls. Finally, the sulfur d orbitals can become part of the conjugated system, and indeed in other contexts sulfur atoms have been shown to be effective at mediating electronic interactions between aromatic rings due to p_π–d_π–p_π overlap.[8] Oligothiophenes are therefore particularly appealing components for use in bridging ligands as it is likely that they will permit strong metal–metal interactions over long distances, but this aspect of their chemistry has received little attention. One recent example was the use of 2,5-di(4-pyridyl)thiophene as a bridging ligand between two $\{Ru(NH_3)_5\}^{2+/3+}$ fragments, where it was found that the electrochemical interaction between the metal centres was somewhat stronger than that across a 1,4-di(4-pyridyl)butadiene bridge which also contains two double bonds between the pyridyl rings.[9]

We describe here the preparation of a series of compounds comprising pyridyl (L^1–L^5) or phenol (H_2L^7) termini at either end of oligothienyl strands, and the synthesis, electrochemical and spectroscopic properties of their complexes containing {Mo[HB(dmpz)$_3$](NO)Cl} groups, and show that these compounds are indeed very effective at transmitting electronic interactions between the remote metal termini.

Experimental

General

The following instrumentation was used for routine spectroscopic studies: ^{1}H NMR spectroscopy, JEOL GX-270, λ-300 or GX-400 spectrometers; electron impact (EI) and fast-atom bombardment (FAB) mass spectra, a VG-Autospec; IR spectra, a Perkin-Elmer FT-1600; UV/VIS spectra, Perkin-Elmer Lambda-2 or -19 instruments; luminescence spectra, a Perkin-Elmer LS-50B instrument. Electrochemical measurements were made with an EG&G PAR 273A potentiostat, using platinum-bead working and auxiliary electrodes, and a saturated calomel reference electrode (SCE). The measurements were performed using acetonitrile distilled over calcium hydride, with 0.1 mol dm^{-3} [NBu$^n_4$][PF$_6$] as supporting electrolyte. Ferrocene was

added at the end of each experiment as an internal reference, and all redox potentials are quoted *vs.* the ferrocene–ferrocenium couple.

The following materials were prepared according to published procedures: 2,2′-bithiophene, 2,2′:5′,2″-terthiophene and 2,2′:5′,2″:5″,2‴-quaterthiophene;[10] 2,5-bis(tri-*n*-butylstannyl)thiophene, 5,5′-bis(tri-*n*-butylstannyl)-2,2′-bithiophene, 5,5″-bis(tri-*n*-butylstannyl)-2,2′:5′,2″-terthiophene and 5,5‴-bis(tri-*n*-butylstannyl)-2,2′:5′,2″:5″,2‴-quaterthiophene;[11] 5,5′-dibromo-2,2′-bithiophene;[12] 4-(tri-*n*-butylstannyl)pyridine.[13]

Ligand syntheses

2,5-Bis(4-pyridyl)thiophene (L^1). To a stirred mixture of 4-bromopyridine (3.60 g, 18.5 mmol; freshly prepared by basification of an aqueous solution of the hydrochloride salt followed by extraction with diethyl ether and evaporation *in vacuo* at 0 °C) and $[Pd(PPh_3)_4]$ (0.60 g, 0.52 mmol) in dry toluene (100 cm^3) was added a solution of 2,5-bis(tri-*n*-butylstannyl)thiophene (4.64 g, 7.00 mmol) in dry toluene (10 cm^3). The reaction mixture was stirred at 100 °C for 16 h before being cooled and treated with saturated aqueous NH_4Cl. The organic layer was separated, and the aqueous residue further extracted with two portions of CH_2Cl_2. The combined organic extracts were dried ($MgSO_4$), the solvents removed, and the residue chromatographed over silica gel by eluting with acetone. The product eluted as the second band which has a strong blue fluorescence. The pure fractions were evaporated to dryness and recrystallised from acetone to give L^1 in 27% yield.

5,5′-Bis(4-pyridyl)-2,2′-bithiophene (L^2). This compound was prepared as described above for L^1 from 4-bromopyridine (3.60 g, 18.5 mmol), $[Pd(PPh_3)_4]$ (0.60 g, 0.52 mmol) and 5,5′-bis(tri-*n*-butylstannyl)-2,2′-bithiophene (6.50 g, 8.77 mmol) in dry toluene (100 cm^3). After cooling, a yellow precipitate formed which was filtered off and recrystallised twice from toluene to give L^2 in 42% yield.

5,5″-Bis(4-pyridyl)-2,2′:5′,2″-terthiophene (L^3). This compound was prepared as described above for L^1 from 4-bromopyridine (1.95 g, 10.0 mmol), $[Pd(PPh_3)_4]$ (0.20 g, 0.17 mmol) and 5,5″-bis(tri-*n*-butylstannyl)-2,2′:5′,2″-terthiophene (2.23 g, 2.70 mmol) in dry toluene (15 cm^3). After cooling, an orange precipitate formed which was filtered off, washed with toluene and recrystallised twice from dimethylformamide to give L^3 in 37% yield.

5,5‴-Bis(4-pyridyl)-2,2′:5′,2″:5″,2‴-quaterthiophene (L^4). This compound was prepared as described above for L^1 from 4-bromopyridine (1.95 g, 10.0 mmol), $[Pd(PPh_3)_4]$ (0.20 g, 0.17 mmol) and 5,5‴-bis(tri-*n*-butylstannyl)-2,2′:5′,2″:5″,2‴-quaterthiophene (1.99 g, 2.20 mmol) in dry toluene (15 cm^3). After cooling, a golden-brown precipitate formed which was filtered off, washed with toluene and dried. A small sample for analytical purposes was recrystallised from hot dimethylformamide, but L^4 is too insoluble to permit bulk recrystallisation. Yield: 39%.

5,5′-Bis[2-(4-pyridyl)ethenyl]-2,2′-bithiophene (L^5). A mixture of 5,5′-dibromo-2,2′-bithiophene (0.78 g, 2.41 mmol), 4-vinylpyridine (1.23 g, 11.7 mmol), palladium(II) acetate (0.028 g, 0.13 mmol) and triphenylphosphine (0.034 g, 0.13 mmol), dry triethylamine (1.5 cm^3) and dry dimethylformamide (2.0 cm^3) was placed in an N_2-purged Schlenk tube which was sealed and heated to 100 °C for 3 d. The contents were stirred throughout. After cooling, the reaction mixture was dissolved in $CHCl_3$ and washed with an aqueous NaCl solution. The residual organic phase was dried ($MgSO_4$) and the concentrated *in vacuo*. The crude solid material was washed with CH_2Cl_2 and then recrystallised from dimethylformamide to give L^5 as a red solid in 45% yield.

5,5′-Bis(4-methoxyphenyl)-2,2′-bithiophene (L^6). To a stirred mixture of 4-bromoanisole (3.74 g, 20.0 mmol) and $[Pd(PPh_3)_4]$ (0.60 g, 0.52 mmol) in dry toluene (100 cm^3) was added a solution of 5,5′-bis(tri-*n*-butylstannyl)-2,2′-bithiophene (6.50 g, 8.77 mmol) in dry toluene (10 cm^3). The reaction mixture was heated to reflux for 16 h and then cooled. The yellow precipitate was filtered off and recrystallised twice from toluene to give the product in 58% yield.

5,5′-Bis(4-hydroxyphenyl)-2,2′-bithiophene (H_2L^7).[14] A mixture of pyridine (technical grade, 15 cm^3) and concentrated HCl (15 cm^3) was heated to 200 °C, whilst maintaining a gentle flow of N_2 gas over the mixture to drive off the steam. When water-free, the mixture started to sublime (white crystals of pyridinium chloride appeared around the neck of the flask) and the molten pyridinium chloride in the flask appeared as a straw-coloured oil. The methylated precursor 5,5′-bis(4-methoxyphenyl)-2,2′-bithiophene (0.50 g, 1.32 mmol) was added and the mixture stirred under N_2 at 190–200 °C for 2 h. After cooling the mixture was dissolved in water (200 cm^3). After standing overnight the precipitated solid was filtered off and washed with water. Recrystallisation from dimethylformamide–water afforded H_2L^7 as a pale green solid in 56% yield.

Characterisation data are in Tables 1 and 2.

Complex preparations

$[\{Mo[HB(dmpz)_3](NO)Cl\}_2(\mu\text{-}L^n)]$ (n = 1–5, 7; complexes 1–5, 7 respectively). A mixture of the appropriate thiophene (0.3 mmol), $[Mo\{HB(dmpz)_3\}(NO)Cl_2]$ (1 mmol) and dry NEt_3 (1 cm^3) in dry toluene (50 cm^3) was heated to reflux for 1–2 d. The reaction may be followed by TLC (silica, CH_2Cl_2): if necessary additional small portions of $[Mo\{HB(dmpz)_3\}(NO)Cl_2]$ were added until the reaction was complete. After concentration to dryness *in vacuo*, the residue was chromatographed on silica using CH_2Cl_2. Unchanged $[Mo\{HB(dmpz)_3\}(NO)Cl_2]$ (orange) and the ubiquitous by-product $[\{Mo[HB(dmpz)_3](NO)Cl\}_2(\mu\text{-}O)]$ (green) were eluted rapidly. Up to 2% tetrahydrofuran (thf) was then added to the CH_2Cl_2 to elute the complexes: **1**–**5** are red-brown and **7** is blue. Details of yields and characterisation data are in Table 3.

Results and Discussion

Ligand syntheses

Compounds L^1–L^4 were prepared by a Pd^0-catalysed cross-coupling between the appropriate bis(tri-*n*-butylstannyl)oligothiophene and 2 equivalents of 4-bromopyridine (Scheme 1). The necessary bis(tri-*n*-butylstannyl)oligothiophene may be prepared in a single step from the parent oligothiophenes. This proved to be a straightforward reaction giving clean products in moderate yields. For L^2–L^4 in particular although the yields are only moderate (≈40% for the cross-coupling reaction) the products are obtained as essentially clean precipitates so work-up and purification is minimal. Compound L^1 was recently prepared by Takahashi and co-workers.[9,16] by a similar method but with the functional groups in the alternative locations, *i.e.* using 2,5-dibromothiophene and 4-(trimethylstannyl)pyridine. This gave a better yield than we obtained, but the advantage of our method for the higher homologues L^2–L^4 is that functionalisation of oligothiophenes with terminal stannyl groups is a straightforward one-pot procedure.[11] The same method was used to prepare the protected *O*-methylated ligand L^6 from 4-bromoanisole and 5,5′-bis(tri-*n*-butylstannyl)-2,2′-bithiophene; demethylation with pyridinium chloride[14] liberated free H_2L^7. Finally, L^5, with ethylenic spacers between the

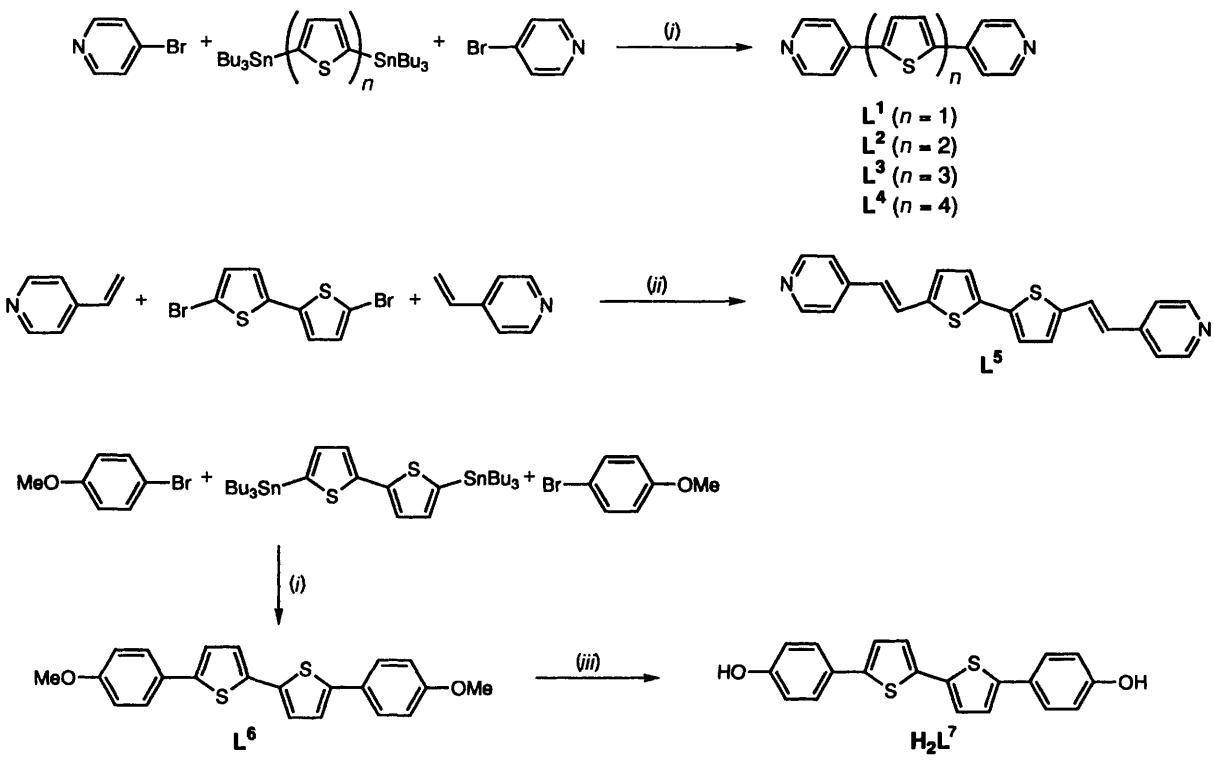

Scheme 1 (*i*) $[Pd(PPh_3)_4]$, toluene, reflux; (*ii*) $[Pd(O_2CMe)_2]$, PPh_3, NEt_3, dmf, 100 °C; (*iii*) pyridinium chloride, 200 °C

terminal pyridyl groups and the bithiophene core, was prepared by a Pd^0-catalysed Heck coupling[17] from 5,5′-dibromo-2,2′-bithiophene and 4-vinylpyridine. All compounds were fully characterised by the usual methods (Table 1). We note that L^1–L^4 were mentioned in a brief communication in which their potential use as laser dyes was evaluated.[18] However the synthetic method is rather cumbersome and low-yielding, and no experimental details were given, nor were the molecules used as ligands.

Electrochemical, spectroscopic and luminescence properties of the ligands

These pyridyl-based compounds are electrochemically active, displaying two chemically reversible one-electron reductions to give radical anion and diradical dianion species, which is the normal behaviour of polythiophenes.[16] For L^1–L^3 the separation between the two reduction potentials ($\Delta E_{\frac{1}{2}}$) decreases steadily as the extent of the conjugated π system increases: this is good evidence for the near-planarity of the molecules in solution. Also, with increasing chain length, the reduction potentials become less negative as the lowest unoccupied molecular orbital (LUMO) is stabilised. Compound L^4 was too insoluble for electrochemical studies to be performed. For L^5 only one broad symmetric reduction wave was observed by cyclic voltammetry: square-wave voltammetry showed the presence of two peaks too closely spaced to allow the individual maxima to be resolved ($\Delta E_{\frac{1}{2}} < 50$ mV), so the presence of the ethylenic spacers considerably reduces the stability of the monoreduced species compared to the doubly reduced species.

For H_2L^7 in contrast no reductions occurred within the accessible potential window, but instead a broad oxidation wave occurred at +0.37 V. The return wave was less intense than the outward wave, indicating some chemical irreversibility. We suggest that this may be a two-electron oxidation to give a quinone species, the electrochemical properties of the complex of L^7 (see later) support this. The irreversibility would then arise from loss of protons on formation of the quinone: in a protic solvent this oxidation would presumably be chemically reversible, like those of other quinones, but H_2L^7 is not sufficiently water soluble to check this. The electrochemical behaviour of L^6 in thf is similar, with no reductions apparent but two oxidation waves centred at $E_{\frac{1}{2}} = +0.44$ and +0.78 V. These are broad ($\Delta E_p \approx 160$ mV in both cases) and poorly resolved, but the cathodic and anodic peak currents are approximately equal. The absence of reductions in H_2L^7 and L^6 is consistent with the terminal hydroxy or methoxy groups acting as strong electron-donating substituents, which will facilitate oxidation and hinder further reduction.

The electronic absorption spectra of the ligands show a strong, relatively low-energy π–π* transition (Table 2). For L^1–L^4 this shifts steadily from 332 to 425 nm as the increasing conjugation of the additional thienyl units reduces the gap between the highest occupied molecular orbital (HOMO) and the LUMO. These parallel the π–π* transitions of the parent oligothiophenes, which vary from 231 nm for thiophene to 385 nm for quaterthiophene,[19] but are at lower energy due to the additional conjugation provided by the pyridyl rings. For L^5 (two thienyl rings and two additional double bonds) the transition is comparable in energy to that of L^4 (four thienyl rings). Compounds L^6 and H_2L^7, with two thienyl rings, have their absorption at essentially the same position as that of L^2 which also has two thienyl rings. The ligands are also intensely luminescent (Table 2). Excitation at the maximum of the π–π* transition results in strong emissions displaying vibrational structure, which in most cases gives two resolved maxima. Sample emission spectra are in Fig. 1. The high quantum yield for L^1 (0.91) is particularly noteworthy; as the ligands increase in length the quantum yield decreases and the emission becomes more red-shifted.

Complex syntheses

Prolonged reaction of each ligand with >2 equivalents of $[Mo\{HB(dmpz)_3\}(NO)Cl_2]$ and NEt_3 in toluene afforded the dinuclear complexes $[\{Mo[HB(dmpz)_3](NO)Cl\}_2(\mu\text{-}L^n)]$ (n = 1–5 or 7, complexes **1**–**5** or **7** respectively) following

Table 1 Analytical and spectroscopic data for the new ligands

Compound	Analysis[a] (%) C	H	N	EI Mass spectrum (m/z for M^+)	^{1}H NMR data[b] (δ, J/Hz)
L^1	70.4 (70.6)	4.3 (4.2)	11.4 (11.7)	238	8.64 (4 H, d, J = 5.8, py H^2/H^6), 7.53 (2 H, s, th H^3/H^4), 7.51 (4 H, d, J = 5.8, py H^3/H^5)
L^2	67.6 (67.5)	3.9 (3.8)	8.3 (8.7)	320	8.60 (4 H, dd, J = 6.4, 1.4, py H^2/H^6), 7.87 (2 H, d, J = 3.7, th $H^4/H^{4'}$), 7.68 (4 H, dd, J = 6.4, 1.4, py H^3/H^5), 7.55 (2 H, d, J = 3.7, th $H^3/H^{3'}$)
L^3	65.2 (65.6)	3.5 (3.5)	6.8 (7.0)	402	*c*
L^4	63.9 (64.4)	3.3 (3.3)	5.6 (5.8)	484	*c*
L^5	70.5 (70.9)	4.7 (4.3)	8.0 (7.5)	372	8.54 (4 H, d, J = 6, py H^2/H^6), 7.75 (2 H, d, J = 16, CH=C*H*), 7.55 (4 H, d, J = 6, py H^3/H^5), 7.38 (2 H, d, J = 3.7, th $H^4/H^{4'}$), 7.32 (2 H, d, J = 3.7, th $H^3/H^{3'}$), 6.95 (2 H, d, J = 16, C*H*=CH)
L^6	70.0 (69.8)	4.9 (4.8)		378	7.53 (4 H, d, J = 8.8, aryl H^2/H^6), 7.12 (4 H, s, th $H^3/H^{3'}/H^4/H^{4'}$), 6.93 (4 H, d, J = 8.8, aryl H^3/H^5)
H_2L^7	68.7 (68.5)	4.1 (4.0)		350	9.72 (2 H, s, OH), 7.48 (4 H, d, J = 8.6, aryl H^2/H^6), 7.29 (2 H, d, J = 3.7, th $H^4/H^{4'}$), 7.24 (2 H, d, J = 3.7, th $H^3/H^{3'}$), 6.81 (4 H, d, J = 8.6, aryl H^3/H^5)

[a] Calculated values in parentheses. [b] Abbreviations: py = pyridyl; th = thienyl. Spectra were recorded at 300 MHz in $(CD_3)_2SO$, except for L^1 and L^6 in $CDCl_3$. [c] Compound too poorly soluble at room temperature to permit an NMR spectrum to be recorded.

Table 2 Electronic spectral, luminescence and electrochemical data for the new ligands

Compound	λ_{max}/nm (10^{-3} ε/dm^3 mol^{-1} cm^{-1})[a]	λ_{em}/nm[a]	φ[b]	$E_{\frac{1}{2}}$[c]/V	$\Delta E_{\frac{1}{2}}$/mV
L^1	332 (33)	385	0.91	−2.15 (90), −2.42 (90)	270
L^2	382 (31)	433, 457	0.11	−2.05 (70), −2.27 (90)	220
L^3	415[d]	479, 503	0.15	−2.02 (90), −2.15 (80)	160
L^4	425[d]	509, 530	0.21	*e*	—
L^5	432 (14)	494, 515	0.13	−1.95 (120)[f]	—
L^6	306 (8.1), 387 (38)	447, 473	0.24	+0.44 (160), +0.78 (170)	340
H_2L^7	308 (5.7), 386 (26)	449, 472	0.14	+0.37 (200)[g]	—

[a] The following (aerated) solvents were used for absorption and emission spectra: L^1, CH_2Cl_2; L^2, L^3 and H_2L^7, dmf; L^4, L^5 and L^6, Me_2SO. [b] Quantum yields were determined using quinine sulfate in 0.5 mol dm^{-3} H_2SO_4 as the standard (φ = 0.546; ref. 15). [c] Electrochemical measurements were made in CH_2Cl_2 containing 0.1–0.2 mol dm^{-3} $NBu^n_4PF_6$ as base electrolyte at a platinum-bead working electrode with a scan rate of 0.1 V s^{-1}. Ferrocene was added as an internal standard at the end of each measurement, and all $E_{\frac{1}{2}}$ values are quoted in volts *vs.* the ferrocene–ferrocenium couple. [d] Owing to the very low solubility of this compound accurate absorption coefficients could not be determined. [e] This compound was too insoluble for electrochemical studies. [f] Two unresolved one-electron processes. [g] Irreversible, assumed to be a two-electron process.

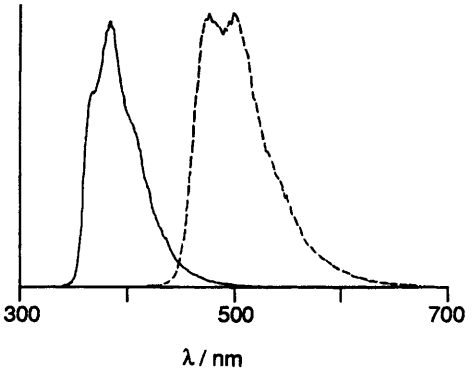

Fig. 1 Uncorrected luminescence spectra of L^1 (solid line) and L^3 (dashed line)

replacement of one chloride at each metal centre by the pyridyl or phenolate ligand; this is a routine reaction which we have discussed before.[3,4] The complexes are numbered in the same way as the bridging ligands; that of L^1 is **1**, and so on. Long reaction times were necessary due to the insolubility of the ligands. Complexes **1–5** therefore contain two {Mo[HB(dmpz)$_3$](NO)Cl(pyridyl)} termini in which the molybdenum groups have a 17 valence-electron configuration and are paramagnetic: if the nitrosyl ligand is assumed to be NO^+ then the Mo is in oxidation state +1. In complex **7**, with {Mo[HB(dmpz)$_3$](NO)Cl(phenolate)} termini, the molybdenum groups have a 16 valence-electron configuration (formally Mo^{2+}) and are diamagnetic.[20] All of the complexes were satisfactorily characterised by FAB mass spectrometry and elemental analyses (Table 3). In addition all complexes had ν(B–H) at *ca.* 2546 cm^{-1} in their IR spectra, together with a characteristic ν(NO) vibration at *ca.* 1608 (**1–5**) and 1680 cm^{-1} (**7**).

Electronic spectra and luminescence of complexes

The electronic spectra of the complexes are dominated by the π–π* transitions of the bridging ligands (Fig. 2, Table 4). The effect of attachment of two molybdenum fragments is to lower the energies of these transitions further: thus the 332 nm absorption of free L^1 moves to 351 nm for complex **1**, indicating that the molybdenum fragments act as net electron acceptors. In energy terms the red-shifts of the π–π* transitions in the pyridyl-based complexes **1–5** are fairly constant (1630, 1730, 1320, 1210 and 1270 cm^{-1} respectively). In contrast, coordination of molybdenum groups to the phenolate termini of L^7 makes little difference to the π–π* transition energy of the bridge. The transition at about 277 nm may be ascribed to a π–π* transition of the terminal tris(pyrazolyl)borate ligands.

For complexes **1–5** we would also expect low-energy metal-to-ligand charge-transfer bands arising from promotion of an electron from a molybdenum d_π orbital to the π* orbital of the pyridyl group.[3] These typically occur in the 450–600 nm region of the spectrum depending on the substituents attached to the pyridyl ligand, and the solvent. As a result they are partly obscured by the low-energy tail of the very strong π–π* transitions of the bridge and are generally only visible as shoulders, so further discussion of them is not warranted. The spectrum of **7** in contrast (Fig. 2, bottom) shows a strong ligand-to-metal (phenolate-to-molybdenum) charge-transfer band at 602 nm. These normally occur at rather higher energy than this; for [Mo{HB(dmpz)$_3$}(NO)Cl(OC$_6$H$_5$)] the phenolate-to-molybdenum charge transfer occurs at 464 nm, and this moves to lower energy as the presence of conjugated

Table 3 Characterisation data for the new complexes

Complex	Yield (%)	M	FAB mass spectrum (m/z) M^+	$M^+ - Cl$	Analysis (%) C	H	N
$[Mo_2L^1]$	38	1155.5	1155	1121	45.6 (45.7)	4.8 (4.7)	19.3 (19.4)
$[Mo_2L^2]$	38	1237.6	1238	1204	46.1 (46.6)	4.7 (4.6)	17.9 (18.1)
$[Mo_2L^3]$	41	1319.7	1318	1283	47.0 (47.3)	4.6 (4.4)	16.9 (17.0)
$[Mo_2L^4]$	28	1401.9	1401	1367	47.9 (48.0)	4.5 (4.3)	15.8 (16.0)
$[Mo_2L^5]$	43	1289.7	1290	1254	48.7 (48.4)	4.8 (4.7)	17.3 (17.4)
$[Mo_2L^7]$	48	1265.6	1265	1230	47.7 (47.5)	4.4 (4.5)	15.0 (15.5)

Table 4 Electrochemical, electronic spectral and luminescence data for the new complexes

Complex	Electronic spectral data[a] λ_{max}/nm ($10^{-3}\varepsilon$/dm^3 mol^{-1} cm^{-1})	Electrochemical data[b] Reductions $E_{\frac{1}{2}}$/V	$\Delta E_{\frac{1}{2}}$[c]/mV	Oxidations $E_{\frac{1}{2}}$/V	Emission data[d] λ_{max}/nm	φ
1	279 (29), 351 (45), 380 (sh),[e] 496 (8.8), 585 (9.1)	−1.60, −2.05	450	+0.07[f]	419, 510 (sh)[e]	0.056
2	279 (24), 409 (48), 520 (12)	−1.68, −1.90	220	+0.07[f]	483, 500 (sh)	0.013
3	277 (41), 439 (78), 490 (sh), 540 (sh)	−1.72, −1.78[g]	60	+0.08[f]	540, 565 (sh)	0.031
4	275 (38), 448 (78), 520 (sh), 570 (sh)	−1.76[f]	—	+0.06[f]	540, 570 (sh)	0.036
5	278 (17), 457 (36), 510 (sh), 560 (sh)	−1.72, −1.77[g]	50	+0.04[f]	550	0.008
7	320 (sh), 381 (58), 602 (33), 750 (sh)	−0.86, −1.53	670	+0.50, +0.68[h]	450, 515	0.010

[a] Measured in CH_2Cl_2. [b] Measurements made in CH_2Cl_2 containing 0.1–0.2 mol dm^{-3} $NBu^n_4PF_6$ as base electrolyte at a platinum-bead working electrode with a scan rate of 0.1 V s^{-1}. Ferrocene was added as an internal standard at the end of each measurement, and all $E_{\frac{1}{2}}$ values are quoted in volts *vs.* the ferrocene–ferrocenium couple. [c] Separation between the two one-electron reduction potentials. [d] Emission spectra were measured in air-equilibrated CH_2Cl_2; quantum yields were determined using $[Ru(bipy)_3][PF_6]_2$ (bipy = 2,2′-bipyridyl) in aerated water as a standard (φ = 0.028, ref. 21). [e] sh = Shoulder: the positions of these are relatively inaccurate (±15 nm). [f] Two coincident one-electron processes. [g] Processes overlapping in cyclic voltammogram; peak potentials were therefore measured by square-wave voltammetry. [h] Separation between the two one-electron oxidation potentials, $\Delta E_{\frac{1}{2}}$ = 180 mV.

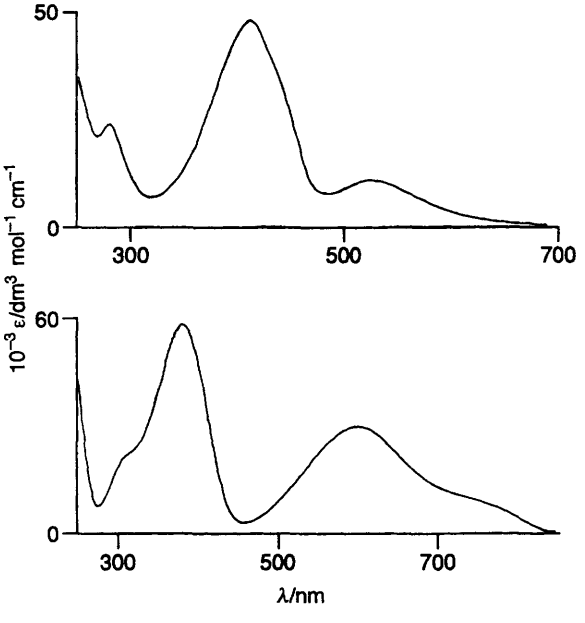

Fig. 2 Electronic spectra of complexes **2** (upper) and **7** (lower) in CH_2Cl_2

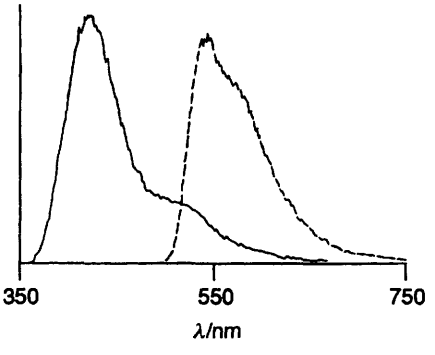

Fig. 3 Uncorrected luminescence spectra of complexes **1** (solid line) and **3** (dashed line) in aerated CH_2Cl_2

substituents on the phenolate ligand raises the HOMO nearer to the empty metal d orbitals. The value of 602 nm for **7** is therefore consistent with effective conjugation between the phenolate termini and the dithienyl core of the bridging ligand.

The complexes are all weakly luminescent (Table 4, Fig. 3). Since {Mo[HB(dmpz)$_3$](NO)Cl(pyridyl)} fragments have no luminescence of their own, it follows that the luminescence originates from the bridging ligands. The emission maxima are all red-shifted compared to those of the free ligands, indicating that we are not just observing emission from traces of free ligand liberated by decomposition of the complexes. This red-shift is consistent with that in the absorption maxima of the ligands when they are attached to the {Mo[HB(dmpz)$_3$](NO)-Cl} fragments and arises from the lowering in energy of the ligand π^* levels following complexation. Some vibrational fine structure is apparent, with at least one pronounced shoulder being apparent on all spectra (Fig. 3). The quantum yields are in the range 0.01–0.05, about an order of magnitude less than those of the free ligands, indicating that most of the luminescence is quenched by the metal centres. Considering the presence of low-energy electronic transitions and redox processes at moderate potentials associated with the metal centres, energy-transfer and electron-transfer quenching pathways are in principle both available.

Electrochemical properties of the complexes

The electrochemical data for the complexes are summarised in Table 4, and confirm that these bridging ligands are very effective at mediating electronic interactions between the metal

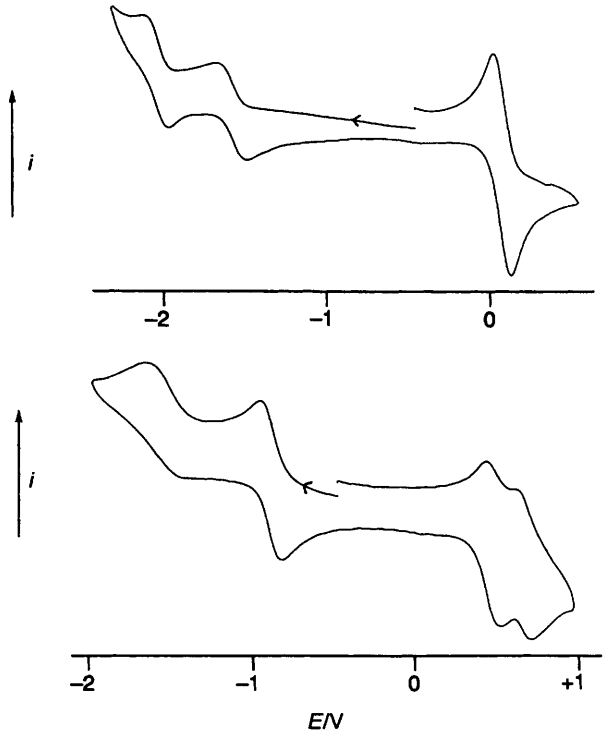

Fig. 4 Cyclic voltammograms of complexes **1** (upper) and **7** (lower) in CH_2Cl_2 at a scan rate of 0.2 V s^{-1}

centres. We will discuss the pyridyl-based complexes **1–5** first. Each 17-electron (17e) {Mo[HB(dmpz)$_3$](NO)Cl(pyridyl)} terminus can undergo a one-electron reduction [formally a Mo^{I}–Mo^{0} couple, giving an 18-electron (18e) configuration] and a one-electron oxidation [formally a Mo^{I}–Mo^{II} couple, giving a 16-electron (16e) configuration].[3,4] In common with all dinuclear complexes of the type [{Mo[HB(dmpz)$_3$](NO)Cl}$_2$(μ-L)], where L is a bis(4-pyridyl) bridging ligand, the two oxidations (which are metal-localised) are coincident, but there is a strong interaction between the two reductions, because they are partly delocalised onto the π* orbitals of the bridging ligand and therefore brought into spatial proximity which will increase the electrostatic interaction between them.[5]

Complexes **1–5** all show, as expected, two reduction processes at potentials characteristic of those of other dinuclear molybdenum complexes with pyridyl-based bridging ligands (Table 4, Fig. 4).[3,4] The particularly low energy of the LUMOs of L^1–L^5 (*cf.* their electronic spectral and electrochemical properties) means that the additional electrons will be even more substantially delocalised onto the bridging ligands than is normally the case: *i.e.* a resonance form in which the bridging ligand is reduced to the dianion will make a significant contribution, and this accounts for the large separations between the reduction potentials. In **1** the splitting of 450 mV between the two reductions may be compared with a splitting of 390 mV between the same metal centres across the bridging ligand 1,4-bis(4-pyridyl)butadiene, which also contains two double bonds between the pyridyl groups. For **2** the splitting of 220 mV exceeds that of 105 mV which occurs across 1,8-bis(4-pyridyl)octatetraene, which also has four double bonds between two 4-pyridyl termini. For **3** the two reduction waves could just be resolved by square-wave voltammetry and are separated by about 60 mV; complex **5**, which also has six double bonds but in the form of two thienyl units and two ethylene units, has a marginally weaker interaction. It is only in **4** with four thienyl groups (eight double bonds) between the pyridyl ligands that the interaction becomes effectively zero (the minimum splitting that can occur in a non-interacting dinuclear complex is 36 mV). This is in contrast to the dipyridylpolyene series, in which the interaction reaches a minimum after five double bonds are inserted between the pyridyl termini.[4] It is clear from these results that bridging ligands containing oligothiophene units are more effective at transmitting electronic interactions than those containing polyene units, due to the combination of factors outlined in the introduction (better delocalisation, less conformational flexibility, lower energy of LUMO).

Complex **7** behaves differently (Fig. 4). The 16-electron {Mo[HB(dmpz)$_3$](NO)Cl(phenolate)} groups do not oxidise at normally accessible potentials, but undergo a one-electron Mo^{II}–Mo^{I} reduction to the 17e state. In dinuclear complexes with bis(phenolate) bridging ligands these two reductions are at different potentials due to an electronic interaction across the bridging ligand,[20] but the lack of a fully conjugated bridging pathway (the phenolate oxygen atoms are formally sp^3 hybridised) means that this interaction is usually weak compared to the interactions across bis(pyridyl) bridging ligands.

The two reductions of complex **7** are separated by a remarkable 670 mV, which is substantially larger than the interaction across the related pyridyl-based ligand in **2** (220 mV). These widely separated reduction processes must involve the bridging ligand, despite the fact that free H_2L^7 did not itself (unlike L^1–L^5) show reductive behaviour at accessible potentials due to the electron-donating effect of the hydroxy groups. It follows that, when co-ordinated to a {Mo[HB(dmpz)$_3$](NO)Cl} centre, each phenolate oxygen becomes less effective at electron donation to the thienyl core, because it is instead donating its electron density to the electron-deficient molybdenum fragment. This effect is apparent in the strong phenolate-to-Mo l.m.c.t. band in the electronic spectrum of **7**, and means that the bridging ligand now behaves more like a conventional oligothiophene group and can be reduced. The very large separation of 670 mV between the reductions must arise (as with **1–5**) because the reduction is substantially delocalised onto the bridging ligand, implying perhaps that the phenolate oxygen atoms are sp^2 rather than sp^3 hybridised so that there can be continuous d_π–p_π–p_π overlap across the Mo–O–aryl fragment. The magnitude of this interaction however is entirely unexpected (it is larger than the 460 mV separation across the much shorter bridging ligand [1,4-$OC_6H_4O]^{2-}$)[20] and we intend to prepare more compounds of this type to clarify the electrochemical behaviour further.

Complex **7** also displays two reversible oxidations, unlike other complexes containing {Mo[HB(dmpz)$_3$](NO)Cl(phenolate)} centres. Considering the electrochemical behaviour of free ligand H_2L^7 and L^6, we ascribe these to oxidations of the bridging ligand which will result in a quinone. Complex **7** is therefore unusual in displaying two different mixed-valence states, and a spectroelectrochemical study of it will be performed in due course.

EPR spectra of the complexes

The EPR spectra of the paramagnetic complexes **1–5** in fluid solution at room temperature are typical of the many other spectra of dinuclear molybdenum complexes in which both metal ions are in the 17e configuration (one unpaired electron).[3,4] In these complexes the modulus of the exchange interaction between the unpaired electrons, $|J|$, is much larger than the hyperfine interaction A_{Mo}, leading to a so-called 'fast-exchange' spectrum in which both electrons are apparently coupled equally to both nuclei. This gives a spectrum centred at $g = 1.978(1)$ consisting of overlapping singlet, sextet and undecet parts arising from coupling to two molybdenum centres which have nuclear spins of either zero (≈75) or $\frac{5}{2}$ (≈25%), with a separation of 2.5(1) mT between the hyperfine components. This is to be expected given that similar spectra arise with a very wide variety of bis(pyridyl) bridging ligands attached to {Mo[HB(dmpz)$_3$](NO)Cl} fragments, and as we have seen, L^1–L^5 are particularly effective at transmitting electronic interactions.

Conclusion

We have prepared a series of six new bridging ligands containing pyridyl or phenol ligating termini and up to four α,α′-linked thienyl groups between them. They are electrochemically active and also strongly luminescent. Their dimolybdenum complexes show electrochemical interactions between the metal centres that are markedly stronger than those across bridging ligands of the same length containing polyene fragments, and show weak emission arising from incomplete quenching of the ligand-based luminescence.

References

1 M. D. Ward, *Chem. Soc. Rev.*, 1995, **24**, 121; *Chem. Ind.*, 1996, **15**, 568.
2 F. L. Carter, *Molecular Electronic Devices II*, Marcel Dekker, New York, 1987; W. Göpel and C. Ziegler (Editors), *Nanostructures Based on Molecular Materials*, VCH, Weinheim, 1992; J.-M. Lehn, *Supramolecular Chemistry*, VCH, Weinheim, 1995; J. M. Tour, *Chem. Rev.*, 1996, **96**, 537.
3 A. J. Amoroso, A. M. W. Cargill Thompson, J. P. Maher, J. A. McCleverty and M. D. Ward, *Inorg. Chem.*, 1995, **34**, 4828; M. M. Bhadbade, A. Das, J. C. Jeffery, J. A. McCleverty, J. A. Navas Badiola and M. D. Ward, *J. Chem. Soc., Dalton Trans.*, 1995, 2769; A. Das, J. C. Jeffery, J. P. Maher, J. A. McCleverty, E. Schatz, M. D. Ward and G. Wollermann, *Inorg. Chem.*, 1993, **32**, 2145; A. Das, J. P. Maher, J. A. McCleverty, J. A. Navas Badiola and M. D. Ward, *J. Chem. Soc., Dalton Trans.*, 1993, 681.
4 S. L. W. McWhinnie, J. A. Thomas, T. A. Hamor, C. J. Jones, J. A. McCleverty, D. Collison, F. E. Mabbs, C. J. Harding, L. J. Yellowlees and M. G. Hutchings, *Inorg. Chem.*, 1996, **35**, 760.
5 J. Bonvoisin, J.-P. Launay, J. A. McCleverty and M. D. Ward, unpublished work.
6 A. M. W. Cargill Thompson, D. Gatteschi, J. A. McCleverty, J. A. Navas, E. Rentschler and M. D. Ward, *Inorg. Chem.*, 1996, **35**, 2701.
7 P. Bäuerle, T. Fischer, B. Bidlingmeier, A. Stabel and J. P. Rabe, *Angew. Chem., Int. Ed. Engl.*, 1995, **34**, 303 and refs. therein; J. Guay, A. Diaz, R. Wu and J. M. Tour, *J. Am. Chem. Soc.*, 1993, **115**, 1869; G. H. Cross, in *Introduction to Molecular Electronics*, eds. M. C. Petty, M. R. Bryce and D. Bloor, Edward Arnold, London, 1995, ch. 5.
8 I. S. Moreira and D. W. Franco, *Inorg. Chem.*, 1994, **33**, 1607; *J. Chem. Soc., Chem. Commun.*, 1992, 450.
9 A.-C. Ribou, J.-P. Launay, K. Takahashi, T. Nihira, S. Tarutani and C. W. Spangler, *Inorg. Chem.*, 1994, **33**, 1325.
10 K. Tamao, S. Kodama, I. Nakajima, M. Kumada, A. Minato and K. Suzuki, *Tetrahedron*, 1982, **38**, 3347.
11 L. L. Miller and Y. Yu, *J. Org. Chem.*, 1995, **60**, 6813.
12 P. Bäuerle, F. Würthner, G. Götz and F. Effenberger, *Synthesis*, 1993, 1099.
13 D. Peters, A.-B. Hornfeldt and S. Gronowitz, *J. Heterocycl. Chem.*, 1990, **27**, 2165.
14 C. Dietrich-Buchecker and J.-P. Sauvage, *Tetrahedron*, 1990, **46**, 503.
15 S. R. Meech and D. Phillips, *J. Photochem.*, 1983, **23**, 193.
16 K. Takahashi and T. Nihira, *Bull. Chem. Soc. Jpn.*, 1992, **65**, 1855.
17 R. F. Heck, *Org. React.*, 1981, **27**, 345.
18 R. Nakajima, T. Ise, Y. Takahashi, H. Yoneda, K. Tanaka and T. Hara, *Phosphorus Sulfur Silicon Relat. Elem.*, 1994, **95–96**, 535.
19 J. W. Sease and L. Zechmeister, *J. Am. Chem. Soc.*, 1947, **69**, 270.
20 S. M. Charsley, C. J. Jones, J. A. McCleverty, B. D. Neaves, S. J. Reynolds and G. Denti, *J. Chem. Soc., Dalton Trans.*, 1988, 293.
21 K. Nakamaru, *Bull. Chem. Soc. Jpn.*, 1982, **55**, 2697.

Received 26*th June* 1996; *Paper* 6/04461A